RESEARCH

Plasma circRNA microarray profiling identifies novel circRNA biomarkers for the diagnosis of ovarian cancer

Lili Ge[1], Yu Sun[1], Yaqian Shi[1], Guangquan Liu[1], Fang Teng[1], Zhe Geng[1], Xiyi Chen[1], Hanzi Xu[2*], Juan Xu[1*] and Xuemei Jia[1*]

Abstract

Background: Circular RNA (circRNA), a class of RNA with a covalent closed circular structure that widely existed in serum and plasma, has been considered an ideal liquid biopsy marker in many diseases. In this study, we employed microarray and qRT-PCR to evaluate the potential circulating circRNAs with diagnostic efficacy in ovarian cancer.

Methods: We used microarray to explore the circRNA expression profile in ovarian cancer patients' plasma and quantitative real-time (qRT)-PCR approach to assessing the candidate circRNA's expression. Then the receiver operating characteristic (ROC) curve was employed to analyze the diagnostic values of candidate circRNAs. The diagnostic model circCOMBO was a combination of hsa_circ_0003972 and hsa_circ_0007288 built by binary logistic regression. Then bioinformatic tools were used to predict their potential mechanisms.

Results: Hsa_circ_0003972 and hsa_circ_0007288 were downregulated in ovarian cancer patients' plasma, tissues, and cell lines, comparing with the controls. Hsa_circ_0003972 and hsa_circ_0007288 exhibited diagnostic values with the Area Under Curve (AUC) of 0.724 and 0.790, respectively. circCOMBO showed a better diagnostic utility (AUC: 0.781), while the combination of circCOMBO and carbohydrate antigen 125 (CA125) showed the highest diagnostic value (AUC: 0.923). Furthermore, the higher expression level of hsa_circ_0007288 in both plasma and ovarian cancer tissues was associated with lower lymph node metastasis potential in ovarian cancer.

Conclusions: Our results revealed that hsa_circ_0003972 and hsa_circ_0007288 may serve as novel circulating biomarkers for ovarian cancer diagnosis.

Keywords: Ovarian cancer, circRNA, Diagnostic biomarker, Plasma

Introduction

Ovarian cancer (OC) is the most malignant female tumor and is estimated to account for approximately 21,410 new cases and 13,770 deaths in 2021 in America [1]. The five-year survival rate of women diagnosed with early localized disease is over 90%, but drops precipitously when diagnosed at stages III or IV (30%) [1]. Notably, the five-year survival rate for stage I OC patients is as high as 92.6%, but only 16.3% of them would be diagnosed within that stage [1]. Therefore, discovering novel biomarkers

*Correspondence: xuhanzi2010@163.com; xujuannj@njmu.edu.cn; xmjia@njmu.edu.cn

[1] Department of Gynecology, Women's Hospital of Nanjing Medical University (Nanjing Maternity and Child Health Care Hospital), 123 Mochou Rd, 210004 Nanjing, China
[2] Department of Radiation Oncology, The Affiliated Cancer Hospital of Nanjing Medical University & Jiangsu Cancer Hospital & Jiangsu Institute of Cancer Research, 210009 Nanjing, China

Ge et al. Journal of Ovarian Research   (2022) 15:58

Page 2 of 12

for OC may be essential for improving the diagnosis and prognosis of OC patients.

At present, protein levels, such as carbohydrate antigen 125 (CA125), Human epididymis protein 4 (HE4), and the algorithms (Risk of Malignancy Index (RMI), and Risk of Ovarian Malignancy Algorithm (ROMA)) which combined CA125 and HE4, are widely applied in the diagnosis and prognosis of OC. However, the sensitivity and specificity of these approaches remain somewhat limited [2–5]. CircRNA, a newly discovered non-coding RNA generated by back-splicing [6], is highly stable (half-life > 48 h) and resistant to exonuclease-mediated RNA decay [7–9]. Its functions have been reported in various diseases, including cancer, where it could regulate cancer's progression via sponging microRNAs (miRNAs), interacting with proteins, regulating transcription or being translation templates [10, 11]. Apart from dictating cancer fate, they are also promising biomarkers for cancer due to their abundance in blood, saliva, and exosomes [12–14].

With the development of high-throughput sequencing and microarray technologies, increasing studies showed that circulating circRNAs had diagnostic or prognostic value in many cancers [15, 16]. CircRNAs are differentially expressed in tumours with different clinical characteristics, suggesting that they may have potential prognostic values. Several investigations have confirmed their prognostic role in different cancers, including OC [17]. Decreased circ-ITCH expression was correlated with the poor prognosis of OC patients [18]. Reduced abundance of hsa_circ_0078607 showed parameters associated with poor prognosis, including advanced FIGO stage and higher serum CA125 level [19]. To date, several studies revealed the diagnostic role of circRNAs in cancer via lipid biopsies [15]. Serum circFoxO3a was downregulated in squamous cervical cancer and correlated with tumor invasion, lymph node metastasis, and poor prognosis [20]. The microarray-based approach has been employed to identify patterns of abnormal circRNA expression in plasma of breast cancer patients, and hsa_circ_0001785 was found as a potentially valuable diagnostic biomarker in breast cancer [21].

Currently, the diagnostic value of circulating circRNAs in OC remains unclear. In this study, we used circRNA microarray, illustrating the circulating circRNA expression profile in plasma of OC patients to find potential diagnostic plasma circRNA biomarkers for OC.

Materials and methods
Patients and samples
The plasma and tissue samples utilized in this study were collected between January 2020 and December 2020 from Women's Hospital of Nanjing Medical University (Nanjing Maternity and Child Health Care Hospital). The clinical characteristics of the patients with plasma samples were shown in Table S1. Two experienced pathologists confirmed the diagnosis of OC through the clinicopathological analysis of surgical tissues. The age-matched benign control (47.9 ± 9.6 versus 52.5 ± 11.8 in OC group) samples were obtained from patients with benign diseases. Moreover, forty-one OC tissues and 15 adjacent tissues were obtained from OC patients (age: 53 ± 7.9 and 50 ± 14.1, respectively). All the plasma samples were collected before treatment, and the tissue samples were collected immediately after surgery. All the samples were stored at -80 °C before use. The Ethics Committee of Nanjing Maternity and Child Health Care Hospital has approved this study (Approval Number: 2021KY-040), and informed consent was obtained from all patients.

Peripheral blood sample collection
Peripheral blood samples (2 ml) were obtained from preoperative patients and controls using BD Vacutainer tubes (New Jersey, USA). Peripheral blood was centrifuged at 3000 rpm for 10 min. The isolated plasma was preserved in the 1.5 mL nuclease-free EP tube and stored at -80℃ until use.

RNA extraction, reverse transcription and quantitative real-time polymerase chain reaction (qRT-PCR)
Total RNA from patients' plasma was extracted using QIAGEN miRNeasy Serum/Plasma Advanced Kit (QIAGEN, Dusseldorf, Germany) according to the manufacturer's instructions. And total RNA from patients' tissue was extracted using GENEJET RNA purification kit (Fermentas, Lithuanin, USA) according to manufacturer's instructions. RNA was reverse transcribed into complementary DNA (cDNA) in a reaction volume of 20 μL using Revert Aid First Strand cDNA Synthesis Kit (Thermo Fisher Scientific, Waltham, USA). qRT-PCR was performed using AceQ Universal SYBR qPCR Master Mix (Vazyme, Nanjing, China) on Applied Biosystems ABI Viia7 (Thermo Fisher Scientific, Waltham, USA). The sequences of the primers used in the PCR assay were listed in Table S2. The levels of circRNAs were calculated using $2^{-\Delta Ct}$ method and GAPDH was used as a control.

RNase R treatment and Sanger sequencing
A total of 3 μg RNA was treated with RNase R as previously described [22]. The control group was treated with nuclease-free water. Then the RNase R treated RNA and control RNA were subjected to cDNA synthesis with random primers according to the instructions for the RevertAid First Strand cDNA Synthesis Kit (Thermo Fisher Scientific, Waltham, USA). The PCR products of the

Ge *et al. Journal of Ovarian Research*   (2022) 15:58

Page 3 of 12

circRNAs were analyzed by sanger sequencing and examined by agarose electrophesis at 120 V for 20 min.

ceRNA microarray

The SBC Human (4 × 180 K) ceRNA array V1.0 (Shanghai Biotechnology Corporation, Shanghai, China) was used to analyze the expression of circRNA. RNAs were extracted from the plasma of four OC patients and four uterine myoma patients as controls by using Serum/Plasma Kit (QIAGEN, Dusseldorf, Germany). Then, NanoDrop ND-1000 instrument (Thermo, Waltham, MA, USA) and Bioanalyzer 2100 (Agilent, Santa Clara, CA, USA) were performed to detect the purity and integrity of the RNA. Total RNAs were amplified and labeled using Low Input Quick Amp Labeling Kit, One-Color (Agilent, Santa Clara, CA, USA) according to the manufacturer's instructions and the labeled complementary RNAs (cRNAs) were purified by RNeasy Mini Kit (QIAGEN, GmbH, Germany). The labeled cRNAs were hybridized using Gene Expression Hybridization Kit (Agilent, Santa Clara, CA, USA). The completed hybridizations were scanned by an Agilent Microarray Scanner (Agilent, Santa Clara, CA, USA), and the Dye channel was set by the software: Green, Scan resolution = 3 μm, PMT 100%, 20 bit. Feature Extraction Software 10.7 (Agilent, Santa Clara, CA, USA) was used to read the data. Finally, quantile normalization and subsequent data processing were performed using the R software package. The screening threshold was set as fold change > 2.0 or < 0.5, P-value < 0.05.

Statistical analysis

SPSS 26.0 (SPSS, Inc., IL, USA) and GraphPad Prism 8.0 (GraphPad, Inc., CA, USA) were used for statistical analysis. Data were compared using Student's t-tests and Man-Whitney tests, as appropriate. The Chi square test was employed to analyze associations between expression of plasma circRNAs and clinical characteristics. The circCOMBO diagnostic model was developed through binary logistic regression analyses. ROC curve analyses were used to determine optimal plasma circRNA expression cutoff values, so that diagnostic utility could be maximized after using SPSS 26.0 to generate ROC curves. The pROC package [23] in R Studio was used to perform DeLong's test between two ROC curves. P-value < 0.05 was considered as statistically significant.

The competing endogenous RNAs (ceRNA) network construction and the identification of hub genes

The miRNA binding sites of the circRNAs were predicted by circInteractome and circBank (Tables S3-S4) [24, 25]. Candidate miRNAs should meet the criteria: highly expressed in OC tissues comparing to normal ovarian tissues (fold change > 1.5, P-value < 0.05). The expression of selected miRNAs was downloaded from GSE47841 (Table S5) [26].

TargetScan [27] and the miRDB [28] database were used to predict the miRNA targeted messenger RNAs (mRNAs). We identified down regulated mRNAs in OC tissues in TCGA database compared with normal ovarian tissues in GTEx database (Table S6). Then the overlap between the downregulated mRNAs and the predicted target mRNAs were obtained, with 137 candidate mRNAs were obtained for further analysis (Table S7).

The Search Tool for the Retrieval of Interacting Genes (STRING) (v11.0) was used to predict the association between candidate miRNAs and mRNAs. A protein-protein interaction (PPI) network was constructed using Cytoscape v3.7.0. The hub genes were selected using the Maximal Clique Centrality (MCC) method. A circRNA-miRNA-hubgene (ceRNA) network was constructed using Cytoscape v3.7.0.

Results

CircRNA expression profile in plasma of OC and control patients

Firstly, circRNA microarray was used to investigate differently expressed circRNAs in the plasma of OC patients and benign individuals. A total of 46 circRNAs were upregulated (red spots), and 595 circRNAs were downregulated (green spots) in OC patients compared with the control (fold change > 2 or < 0.5 and P-value < 0.05) (Fig. S1 and Table S8).

Validation of candidate circRNA expression

To validate the microarray results, four candidate circRNAs (hsa_circ_0053221, hsa_circ_0062215, hsa_circ_0003972, hsa_circ_0007288) with the following criteria: (1) high normalized signal (2) fold-change > 2 or < 0.5 and P-value < 0.01, were randomly selected. The head-to-tail splicing of these circRNAs was further analyzed by RNase R treatment and Sanger sequencing. All these four circRNAs were resistant to RNase, while their liner compartments were sensitive to RNase R (Fig S2a-d, left), which indicated the existence of these circRNAs. Compared with hsa_circ_0003972 and hsa_circ_0007288, the expression of hsa_circ_0053221 and hsa_circ_0062215 were relatively low, as shown in both the microarray data and the qRT-PCR results (Table S8 and Fig S2a-b, left). In addition, head-to-tail splicing was validated by sanger sequencing of the qRT-PCR products (Fig S2a-d, right). We next evaluated the expression of these circRNAs in plasma samples from 60 OC patients and 60 benign patients to validate the clinical relevance of these circRNAs. The results indicated that hsa_circ_0003972 and hsa_circ_0007288 were downregulated

in the plasma of OC patients, comparing with benign controls, which were consistent with the microarray results (Fig S2e-f). Meanwhile, hsa_circ_0053221 and hsa_circ_0062215 were undetermined in more than half of the plasma samples, which led to unreliable results. Hence, we selected hsa_circ_0003972 and hsa_circ_0007288 for further analysis.

Correlation between candidate circRNAs expression and clinical characteristics

Then we analyzed the correlation between the expression of these two circRNAs in the benign control group (uterine fibroids versus other benign diseases) and found that the expression levels of these two candidate circRNAs showed no significant difference between uterine fibroids and other benign diseases (Table S9), which could exclude the possible influence of the proliferative characteristic of uterine fibroids. The 60 OC patients were divided into two groups based on the median expression levels of circRNA: high ($n = 30$) and low ($n = 30$) groups. Then we assessed the correlation between plasma levels of these two candidate circRNAs and the clinical characteristics of OC patients (Table 1). The results showed

that the expression of plasma hsa_circ_0007288 was only significantly associated with lymph node metastasis ($P = 0.02$). And the plasma level of hsa_circ_0003972 was not significantly associated with all the clinical characteristics we analyzed.

The diagnostic performance of the two candidate circRNAs in OC

Then, the ROC curve analysis was used to investigate the diagnostic values of these two candidate circRNAs. As shown in Fig. 1a-b; Table 1, the ROC curve showed that hsa_circ_0003972 had an AUC of 0.724 (95% CI: 0.632–0.815), and hsa_circ_0007288 had an AUC of 0.790 (95% CI: 0.705–0.875) in distinguishing OC patients from benign individuals. We next established a diagnostic model consisted of these two circRNAs (circCOMBO) using binary logistic regression analysis. The AUC, sensitivity, and specificity of circCOMBO in distinguishing OC and benign control patients were 0.781 (95% CI: 0.696–0.867), 66.7%, and 86.7%, respectively (Fig. 1c-d; Table 2). The Z test was used to compare the AUC of two circRNAs with that of circCOMBO. We found that the diagnostic

Table 1 The correlation between the expression of plasma circRNAs and clinical characteristics of ovarian cancer patients

Variables	circ-0003972		P	circ-0007288		P
	low expression	high expression		low expression	high expression	
Age			0.605			1
≤53	16	14		15	15	
>53	14	16		15	15	
Menopausal Stage			0.292			0.598
pre-M	14	10		13	11	
post-M	16	20		17	19	
Ovarian Cancer type			0.519			0.519
EOC	23	25		25	23	
others	7	5		5	7	
FIGO Stage			0.787			0.284
I-II	10	11		9	13	
III-IV	20	19		21	17	
Lymphatic metastasis			0.559			0.02
No	23	21		18	26	
Yes	7	9		12	4	
Distant metastasis			0.612			0.612
No	27	29		27	29	
Yes	3	1		3	1	
Histological grade			0.785			0.243
Low	7	9		10	6	
High	21	23		20	24	
CA125(U/mL)			1			0.559
≤35	8	8		9	7	
>35	22	22		21	23	

Ge *et al. Journal of Ovarian Research* (2022) 15:58

Page 5 of 12

Fig. 1 The diagnostic performance of circ_0003972, hsa_circ_0007288, and circCOMBO. **a** ROC curve analysis for the diagnostic performance of hsa_circ_0003972. **b** ROC curve analysis for the diagnostic performance of hsa_circ_0007288. **c** ROC curve analysis for the diagnostic performance of circCOMBO. **d** The diagnostic performance of hsa_circ_0003972, hsa_circ_0007288, and circCOMBO
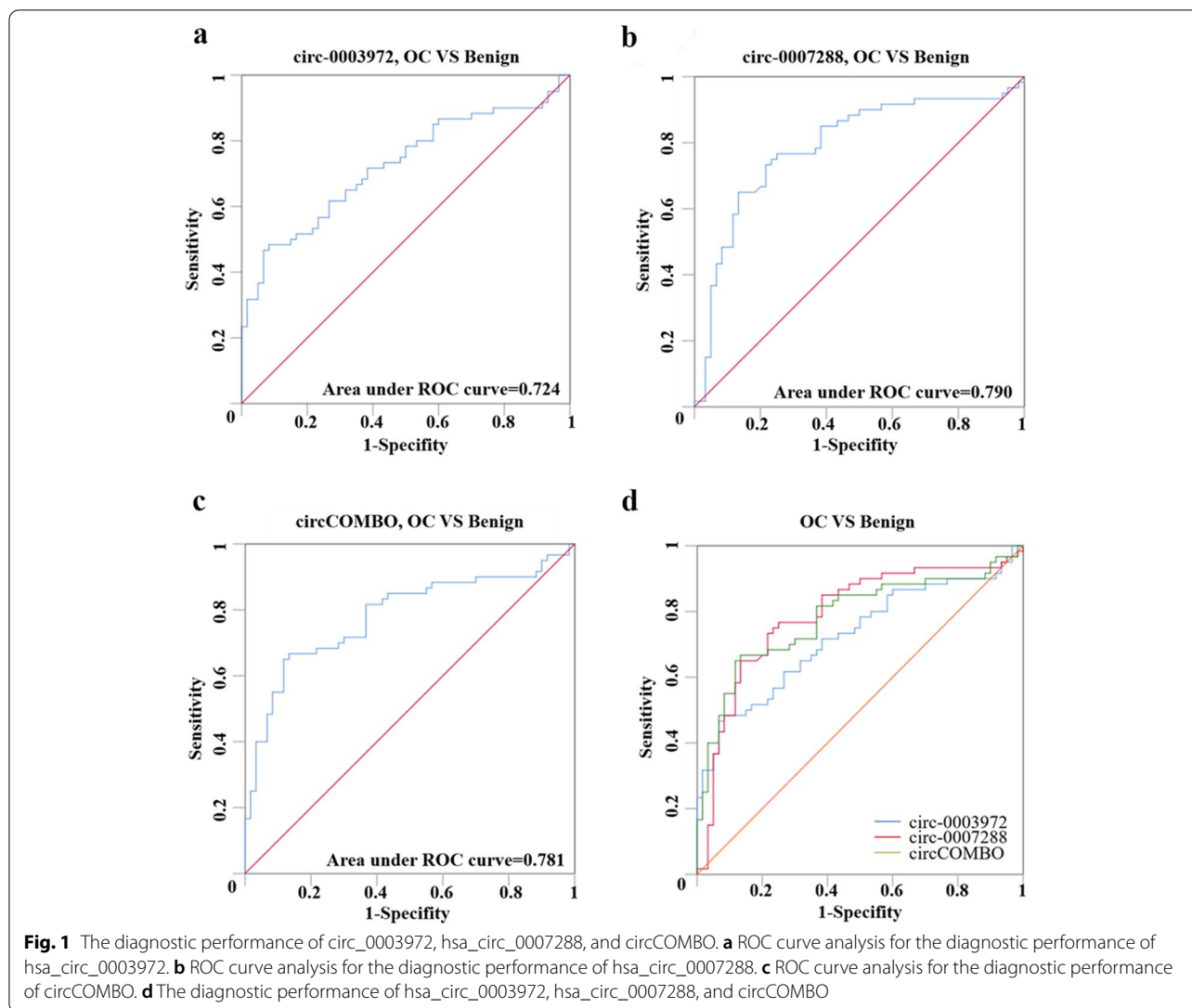
Table 2 The performance of two candidate circRNAs and circCOMBO for the diagnosis of ovarian cancer

Groups	Best cut-off	AUC(95%CI)	Sensitivity(%)	Specificity(%)	*P*-value	Comparison of AUC	
						Groups	*P*-value
circ-0003972	0.26	0.724(0.632–0.815)	48	92	$p < 0.0001$	circ-0003972 vs. circ-0007288	0.2261
circ-0007288	0.011	0.790(0.705–0.875)	77	75	$p < 0.0001$	circ-0003972 vs. circCOMBO	0.0322
circCOMBO	0.45	0.781(0.696–0.867)	66.7	86.7	NA	circ-0007288 vs. circCOMBO	0.8210

utility of circCOMBO was better than that of hsa_circ_0003972, while there was no difference between hsa_circ_0003972 and hsa_circ_0007288, or between circCOMBO and hsa_circ_0007288 for the diagnosis of OC patients (Table 2).

The diagnostic performance of circRNA and/or CA125 in the detection of OC

CA125 has been the most commonly used diagnostic marker of OC patients. Therefore, we further studied the combined diagnostic value of hsa_circ_0003972,

Ge *et al. Journal of Ovarian Research*   (2022) 15:58

Page 6 of 12

hsa_circ_0007288, or circCOMBO with CA125(AUC: 0.824 (95%CI: 0.739–0.908)) in differentiating OC from benign controls. The results showed that the diagnostic performance of CA125+hsa_circ_0007288, CA125+hsa_circ_0003972, CA125+circCOMBO were better than hsa_circ_0007288, hsa_circ_0003972, circCOMBO or CA125 alone, and CA125+circCOMBO had the highest diagnostic value. However, there was no significant difference between CA125+hsa_circ_0007288, CA125+hsa_circ_0003972 and CA125+circCOMBO (Fig. 2; Table 3 and Table S10).

Relative expression of circRNAs in OC tissues and cell lines
We hypothesized that the two candidate circRNAs might also be involved in OC development since hsa_circ_0007288 was significantly associated with lymph node metastasis. To verify our presumptions, we used qRT-PCR to confirm the expression patterns of the two selected circRNAs in OC tissues, OC cell lines (A2780 and SKOV3), normal ovarian tissues, and normal ovarian epithelial cell line IOSE386, and found that both of these two circRNAs were downregulated in OC tissues ($n=41$) and OC cell lines as compared with adjacent tissues ($n=15$) (Fig. 3a-b) and IOSE386 (Fig. 3c-d), respectively. We also analyzed the correlation between the tissue levels of two circRNAs and the clinical characteristics of OC patients (Table 4). Interestingly, we found that the expression of hsa_circ_0007288 was negatively correlated with lymph node metastasis while hsa_circ_0003972 wasn't related to any clinical characteristics, which is similar with the results in the plasma level.
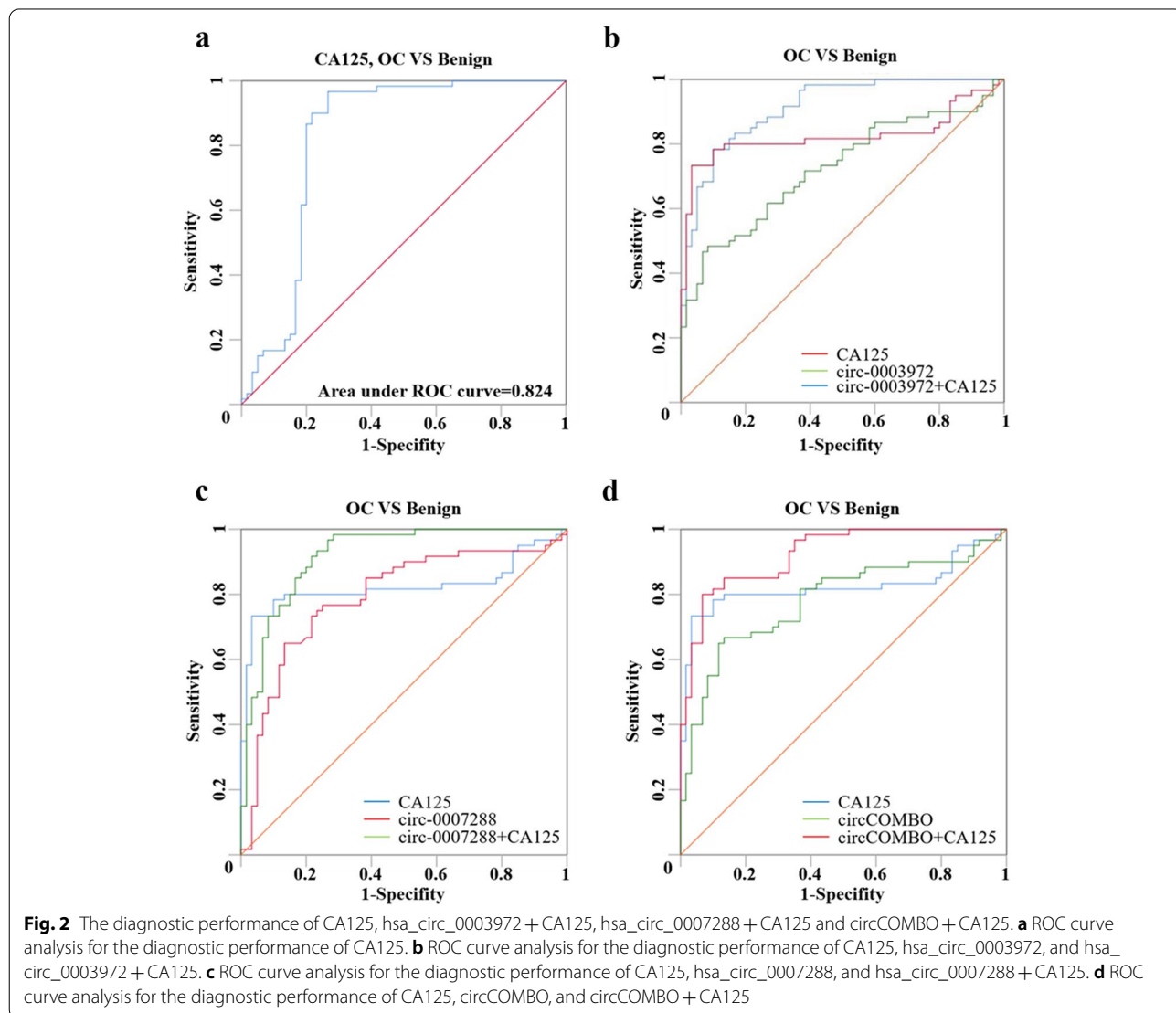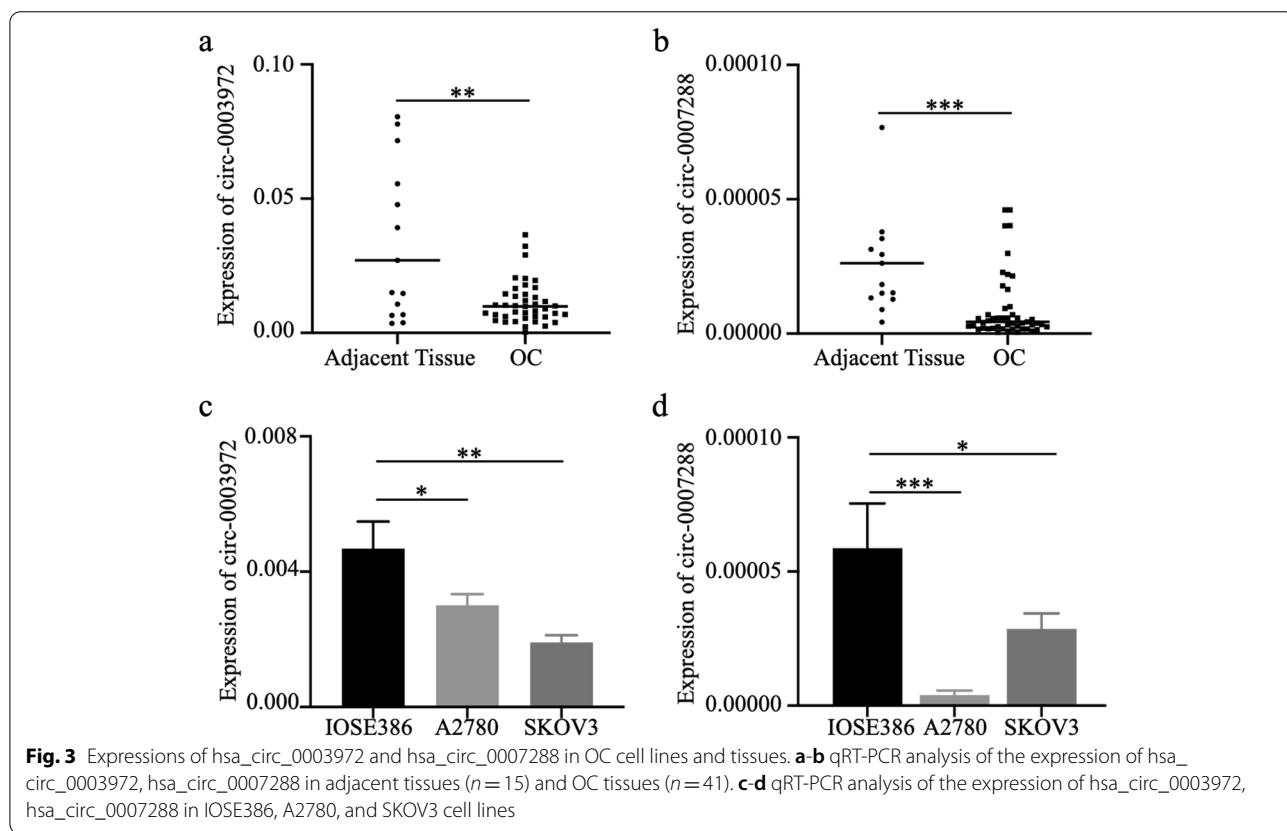

Fig. 2 The diagnostic performance of CA125, hsa_circ_0003972 + CA125, hsa_circ_0007288 + CA125 and circCOMBO + CA125. **a** ROC curve analysis for the diagnostic performance of CA125. **b** ROC curve analysis for the diagnostic performance of CA125, hsa_circ_0003972, and hsa_circ_0003972 + CA125. **c** ROC curve analysis for the diagnostic performance of CA125, hsa_circ_0007288, and hsa_circ_0007288 + CA125. **d** ROC curve analysis for the diagnostic performance of CA125, circCOMBO, and circCOMBO + CA125

Ge *et al. Journal of Ovarian Research*   (2022) 15:58

Page 7 of 12

Table 3 The diagnostic performance and the comparison between the diagnostic performance of CA125, hsa_circ_0003972 + CA125, hsa_circ_0007288 + CA125 and circCOMBO + CA125

	Best cut-off	AUC(95%CI)	Sensitivity (%)	Specificity (%)	*P*-value	Comparison of AUC	
						Groups	*P*-value
CA125	38.825U/ml	0.824(0.739–0.908)	97	73	*p* < 0.0001		
CA125 + circ-0003972	—	0.912(0.864–0.961)	78.3	90.0	NA	circ-0003972 vs. CA125	0.1201
						circ-0003972 vs. circ-0003972 + CA125	*p* < 0.0001
						CA125 vs. circ-0003972 + CA125	0.0781
CA125 + circ-0007288	—	0.918(0.869–0.968)	98.3	71.7	NA	circ-0007288 vs. CA125	0.5839
						circ-0007288 vs. circ-0007288 + CA125	0.0011
						CA125 vs. circ-0007288 + CA125	0.0613
CA125 + circCOMBO	—	0.923(0.878–0.968)	80.0	93.3	NA	circCOMBO vs. CA125	0.4947
						circCOMBO vs. circCOMBO + CA125	*p* < 0.0001
						CA125 vs. circCOMBO + CA125	0.0449

Fig. 3 Expressions of hsa_circ_0003972 and hsa_circ_0007288 in OC cell lines and tissues. **a-b** qRT-PCR analysis of the expression of hsa_circ_0003972, hsa_circ_0007288 in adjacent tissues (*n* = 15) and OC tissues (*n* = 41). **c-d** qRT-PCR analysis of the expression of hsa_circ_0003972, hsa_circ_0007288 in IOSE386, A2780, and SKOV3 cell lines

Construction of the ceRNA network

As hsa_circ_0003972 and hsa_circ_0007288 were significantly downregulated in OC patients, we chose six miRNAs (hsa-miR-1228-3p, hsa-miR-1825, hsa-miR-183-5p (also named as hsa_miR_183-5p.1), hsa-miR-203, hsa-miR-421, hsa-miR-935) which harbored at least one binding site in either of these two circRNAs and were significantly upregulated in OC patients to construct the circRNA-miRNA-mRNA network. A total of 14,086 and 4239 target mRNAs of the six miRNAs were predicted

Ge *et al. Journal of Ovarian Research*   (2022) 15:58

Page 8 of 12

Table 4 The correlation between the expression of tissue circRNAs and clinical characteristics of ovarian cancer patients

Variables	circ-0003972		P	circ-0007288		P
	low expression	high expression		low expression	high expression	
Age			0.155			0.867
≤53	9	13		10	9	
>53	12	7		11	11	
Menopausal Stage			0.153			0.91
pre-M	5	9		7	7	
post-M	16	11		14	13	
FIGO Stage			0.853			0.212
I,II	9	8		7	11	
III,IV	12	12		14	10	
Lymphatic metastasis			0.248			0.037
No	11	14		9	15	
Yes	10	6		12	5	
Distant metastasis			0.37			0.954
No	17	19		19	17	
Yes	4	1		2	3	
Histological grade			0.651			0.651
Low	4	6		4	6	
High	17	14		17	14	
CA125(U/mL)			0.954			0.954
≤35	2	3		2	3	
>35	19	17		19	17	

by TargetScan and miRDB, respectively. Compared with normal ovarian tissues in GTEx database, 2919 mRNAs were downregulated in OC tissues in TCGA database. After taking intersections of these predicted and downregulated mRNAs, 137 mRNAs were selected as the targets of the six miRNAs for further analysis.
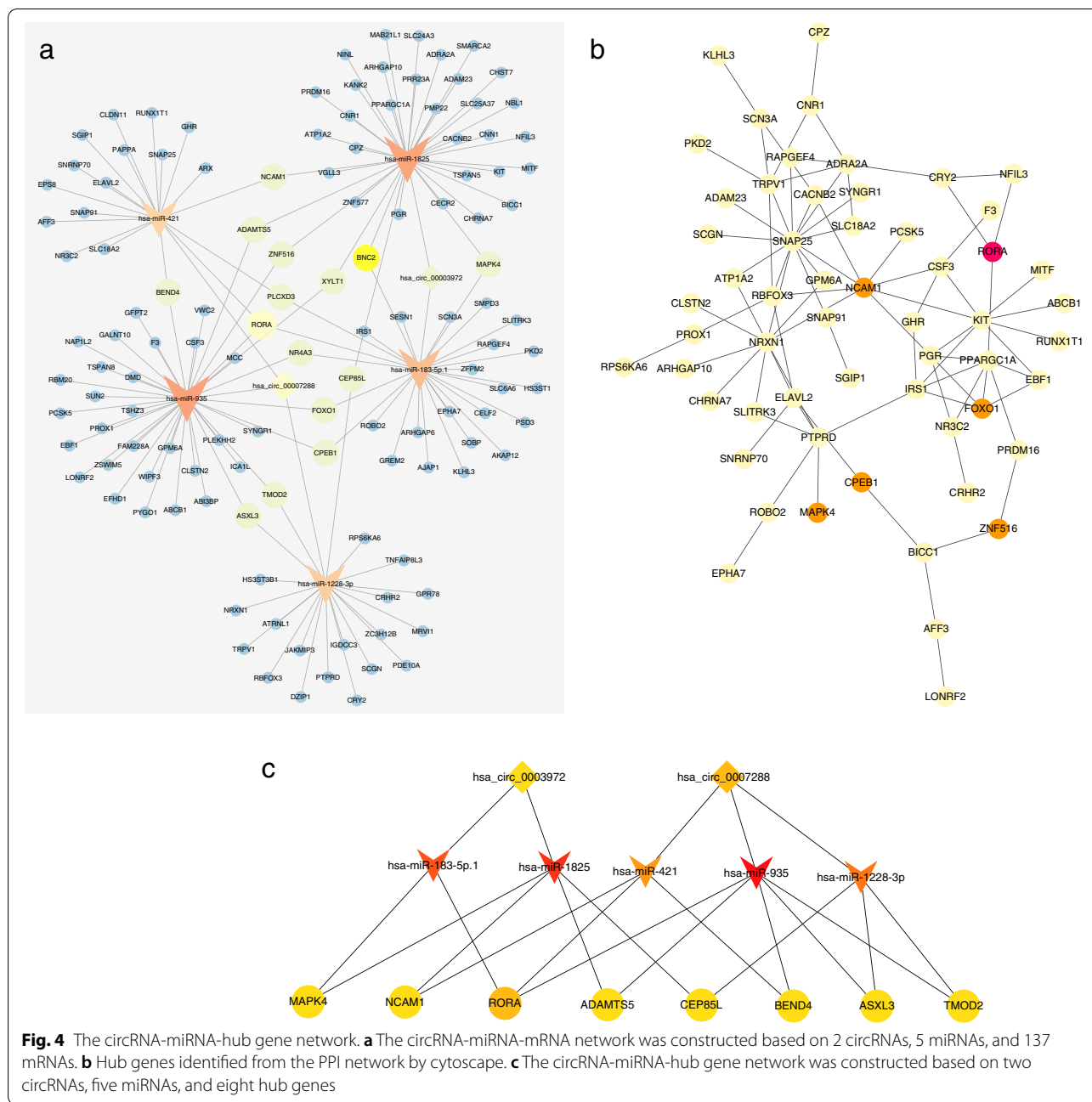
During the construction of the circRNA-miRNA-mRNA network, hsa-miR-203 failed to link with other miRNAs and mRNAs. Therefore, two circRNAs, five miRNAs, and 137 mRNAs were seen in the ceRNA network (Fig. 4a). We used the STRING database to build a PPI network composed of the 137 overlapping mRNAs (Fig. 4b). The hub genes were identified using the MCC method in Cytoscape, and the circRNA-miRNA-hub gene network was visualized by cytoscape (Fig. 4c).

Discussion

CircRNA in cancer mainly functions through sponging miRNAs [29], interacting with proteins [30], or encoding peptides [31, 32]. Its high stability in body fluids and different expression in cancer made them ideal cancer biomarkers [13, 33–35]. It has been reported that plasma hsa_circ_0001785 could be a diagnostic biomarker for breast cancer [21], plasma hsa_circ_0005927, hsa_circ_0001900, hsa_circ_0001178 for colorectal

cancer [36] and plasma circFoxO3a for cervical cancer [20]. However, only plasma circBNC2 (hsa_circ_0008732) has been reported as a diagnostic biomarker in OC patients [37, 38], and the circRNA expression profile in the plasma of OC patients has not been studied yet. Hence, we employed microarray to further identify the potential diagnostic circRNAs in the plasma of OC patients. Our results indicated that hsa_circ_0003972 and hsa_circ_0007288 may serve as important diagnostic biomarker of OC, while circBNC2 (hsa_circ_0008732), the known diagnostic biomarker in the plasma of OC patient, was not detected by microarray in our study and couldn't be detected in most of our plasma samples by qRT-PCR, which indicated that its expression is very low, at least lower than hsa_circ_0003972 and hsa_circ_0007288. Furthermore, qRT-PCR indicated that its expression was comparable between ovarian cancer cell lines and normal ovarian epithelial cell lines (data not shown).

In this study, we also confirmed that the novel circRNAs: hsa_circ_0003972 and hsa_circ_0007288 are downregulated in both the OC tissues and the plasma of OC patients as compare with the adjacent normal ovarian tissues and the plasma of patients with benign disease, indicating that they may produce from normal tissues/cells and perform as the regulator of OC progression.

Fig. 4 The circRNA-miRNA-hub gene network. **a** The circRNA-miRNA-mRNA network was constructed based on 2 circRNAs, 5 miRNAs, and 137 mRNAs. **b** Hub genes identified from the PPI network by cytoscape. **c** The circRNA-miRNA-hub gene network was constructed based on two circRNAs, five miRNAs, and eight hub genes

And their down-regulation in the plasma or tissue levels of ovarian cancer patients was possibly caused by the suppression of the oncogenic RNA binding proteins, such as in DHX9 and ADAR1 [39–41]. CeRNAs are RNA transcripts that can regulate each other through miRNA response elements [29]. miRNAs have proven as robust biomarkers in gynecological cancers, including cervical cancer [42], endometrial cancer [43] as well as OC [44]. Increasing evidence has suggested that circRNAs may perform their functions by acting as ceRNAs [45].

Their interactions indicated approachable fields for early detection and prognosis of cancer [46]. Circular RNA ciRS-7 acted as a sponge of miR-7, upregulating several oncogenes (mTOR, EGFR, PIK3CD) to promote the progression of cancers in which high ciRS-7 expression correlated with worse prognosis and miR-7 acted as tumor suppressor [47–50]. Circular RNA itchy E3 ubiquitin protein ligase (circ-ITCH) has proven to be a suppressor in various cancers such as melanoma and OC [51]. Its high expression was an independent prognostic biomarker of

OC. Meanwhile, it can also function by sponging miR-106a and thereby suppressing OC cell proliferation and invasion [18, 52]. Using bioinformatics analysis, we found that two differentially expressed circRNAs may sponge five different miRNAs. Previous studies have shown that miR-183-5p exerted an oncogenic function in breast cancers [53] and could be a prognostic biomarker of OC [54]. It has been reported that miR-421, miR-935, and miR-1825 promoted the progression of glioblastoma, osteosarcoma, and liver cancer, respectively [55–57], and high expression of serum miR-1228-3p was related to poor prognosis of non-small cell lung cancer [58].

We selected downregulated genes in TCGA OC database to establish a circRNA-miRNA-hub gene network, while MAPK4, NCAM1, RORA, ADAMTS5, CEP85L, BEND4, ASXL3, TMOD2 were considered as the hub genes. Interestingly, RORA, acting as a potent tumor suppressor, was downregulated in several cancers, such as breast cancer and colorectal cancer, which inhibited cancers' growth through attenuating Wnt/beta-catenin signaling, inducing SEMA3F expression or stabilizing p53 to activate apoptosis [59–61]. ADAMTS5, a zinc metalloprotease, has been involved in many biological processes, including inflammation, angiogenesis, and tumorigenesis [62]. Overexpressed MAPK4 was correlated with poor survival in various cancers [63] and played an oncogenic role in prostate cancer [64]. NCAM1 helped cancer cell's perineural invasion [65] and promoted leukemogenesis and drug resistance in acute myeloid leukemia [66]. However, no studies demonstrated the role of ASXL3, TMOD2, and CEP85L in cancer. Based on the above studies, we speculated that both hsa_circ_0003972 and hsa_circ_0007288 may also act as tumor suppressors in OC through sponging the oncogenic miRNAs, thereby regulating target genes' expression. Indeed, hsa_circ_0003972 was also detected in PBMC of Rheumatoid Arthritis patients, and suppressing the expression of hsa_circ_0003972 could inhibit the progression of Rheumatoid Arthritis at least partially through anti-inflammatory effect [67–69]. Besides, hsa_circ_0003972 mainly exerted its function in Rheumatoid Arthritis as the miRNA sponger [68, 69]. However, the exact role of hsa_circ_0003972 and hsa_circ_0007288 in ovarian cancer progression should be illustrated by extensive *in vitro* and *in vivo* studies in the future.

Although the exact mechanisms of the two identified circRNAs in OC were unknown, our results helped to underline the potential mechanisms of their pathogenesis in OC. Besides, examination of the circRNA's expression in tissues may also provide the clue to derivation of circRNAs and point out the potential systemic effect.

Conclusions

Our research revealed that novel plasma circRNA hsa_circ_0003972 and hsa_circ_0007288, the combination of hsa_circ_0003972 and hsa_circ_0007288 (circ-COMBO), the combination of circCOMBO and CA125 could serve as a novel circulating biomarker for OC diagnosis. Meanwhile, the combination of circCOMBO and CA125 showed the highest diagnostic performance. The lower plasma level of hsa_circ_0007288 could serve as a potential biomarker for OC lymph node metastasis. Besides, hsa_circ_0003972 and hsa_circ_0007288 may also become the potential therapeutic target of OC.

Abbreviations
circRNA: Circular RNA; OC: Ovarian cancer; qRT-PCR: Quantitative real-time Polymerase Chain Reaction; ROC: Receiver operating characteristic; AUC: Area Under Curve; CA125: Carbohydrate antigen 125; HE4: Human epididymis protein 4; RMI: Risk of Malignancy Index; ROMA: Risk of Ovarian Malignancy Algorithm; cDNA: Complementary DNA; ceRNA: Competing endogenous RNAs; PPI: Protein-protein interaction; STRING: The Search Tool for the Retrieval of Interacting Genes; MCC: Maximal Clique Centrality.

Supplementary information
The online version contains supplementary material available at https://doi.org/10.1186/s13048-022-00988-0.

Additional file 1: Figure S1. CircRNA expression profiles in OC patients and benign individuals. The expression profile detected by circRNA microarray assay was shown in volcano plot. Four OC patients and four benign individuals were enrolled. Red spots indicated upregulated circRNAs and green spots indicated downregulated circRNAs.

Additional file 2: Figure S2. Validation of the four candidate circRNAs. (a-d). (Left): The electrophoresis of the qRT-PCR product of circRNA and linear RNA treated with or without RNase R. (Right): Sanger sequencing of the RT-PCR product in the left, and the base in the red square represented the head-to-tail splicing sites. (e-f). qRT-PCR analysis of the expression of hsa_circ_0003972, hsa_circ_0007288 in 60 OC patients and 60 benign controls' plasma.

Additional file 3: Table S1. Clinicopathological characteristics of the enrolled patients. **Table S2.** Primer sequences for real-time PCR or quantitative real-time PCR. **Table S3.** The miRNA target prediction software circInteratome and circbank predicted miRNAs which could bind hsa_circ_0003972. **Table S4.** The miRNA target prediction software circInteratome and circbank predicted miRNAs which could bind hsa_circ_0007288. **Table S5.** The expression profile of the miRNAs that were upregulated in OC tissues as compared with normal ovarian tissues downloaded from GSE47841. **Table S6.** The downregulated mRNAs in OC tissues in TCGA database compared with normal ovarian tissues in GTEx database. **Table S7.** The 137 candidate mRNAs expression pattern in OC tissues as compared with normal ovarian tissues. **Table S8.** The microarray results of the 46 upregulated circRNAs and 595 downregulated circRNAs in OC patients compared with the benign control (fold change > 2 and *P*-value < 0.05). **Table S9.** The expression difference of candidate circRNAs between patients with uterine myoma or other benign diseases. **Table S10.** Comparison of AUC in circ-0003972 + CA125, circ-0007288 + CA125, circCOMBO + CA125.

Declarations

Ethics approval and consent to participate
This study has been approved by the Ethics Committee of Nanjing Maternity and Child Health Care Hospital (approval number: 2021KY-040). Written consent was obtained from the patients involved in this study.

Consent for publication
The authors confirm that human research participants provided informed consent for publication of the images and tables.

Competing interests
The authors declare that there are no competing interests.

References

1. Siegel RL, Miller KD, Fuchs HE, Jemal A. Cancer Statistics, 2021. CA Cancer J Clin. 2021;71(1):7–33.
2. Bast RC, Feeney M, Lazarus H, Nadler LM, Colvin RB, Knapp RC. Reactivity of a monoclonal antibody with human ovarian carcinoma. J Clin Invest. 1981;68(5):1331–7.
3. Hellström I, Raycraft J, Hayden-Ledbetter M, Ledbetter JA, Schummer M, McIntosh M, et al. The HE4 (WFDC2) protein is a biomarker for ovarian carcinoma. Cancer Res. 2003;63(13):3695–700.
4. Chudecka-Głaz AM. ROMA, an algorithm for ovarian cancer. Clin Chim Acta. 2015;440:143–51.
5. Jacobs I, Oram D, Fairbanks J, Turner J, Frost C, Grudzinskas JG. A risk of malignancy index incorporating CA 125, ultrasound and menopausal status for the accurate preoperative diagnosis of ovarian cancer. Br J Obstet Gynaecol. 1990;97(10):922–9.
6. Vincent HA, Deutscher MP. Substrate recognition and catalysis by the exoribonuclease RNase R. J Biol Chem. 2006;281(40):29769–75.
7. Jeck WR, Sorrentino JA, Wang K, Slevin MK, Burd CE, Liu J, et al. Circular RNAs are abundant, conserved, and associated with ALU repeats. RNA. 2013;19(2):141–57.
8. Li J, Sun D, Pu W, Wang J, Peng Y. Circular RNAs in Cancer: Biogenesis, Function, and Clinical Significance. Trends Cancer. 2020;6(4):319–36.
9. Salzman J, Chen RE, Olsen MN, Wang PL, Brown PO. Cell-type specific features of circular RNA expression. PLoS Genet. 2013;9(9):e1003777.
10. Yang X, Mei J, Wang H, Gu D, Ding J, Liu C. The emerging roles of circular RNAs in ovarian cancer. Cancer Cell Int. 2020;20:265.
11. Shi Y, He R, Yang Y, He Y, Shao K, Zhan L, et al. Circular RNAs: Novel biomarkers for cervical, ovarian and endometrial cancer (Review). Oncol Rep. 2020;44(5):1787–98.
12. Zhang SJ, Chen X, Li CP, Li XM, Liu C, Liu BH, et al. Identification and Characterization of Circular RNAs as a New Class of Putative Biomarkers in Diabetes Retinopathy. Invest Ophthalmol Vis Sci. 2017;58(14):6500–9.
13. Li Y, Zheng Q, Bao C, Li S, Guo W, Zhao J, et al. Circular RNA is enriched and stable in exosomes: a promising biomarker for cancer diagnosis. Cell Res. 2015;25(8):981–4.
14. Bahn JH, Zhang Q, Li F, Chan T-M, Lin X, Kim Y, et al. The landscape of microRNA, Piwi-interacting RNA, and circular RNA in human saliva. Clin Chem. 2015;61(1):221–30.
15. Wang S, Zhang K, Tan S, Xin J, Yuan Q, Xu H, et al. Circular RNAs in body fluids as cancer biomarkers: the new frontier of liquid biopsies. Mol Cancer. 2021;20(1):13.
16. Wei G, Zhu J, Hu H-B, Liu J-Q. Circular RNAs: Promising biomarkers for cancer diagnosis and prognosis. Gene. 2021;771:145365.
17. Sheng R, Li X, Wang Z, Wang X. Circular RNAs and their emerging roles as diagnostic and prognostic biomarkers in ovarian cancer. Cancer Lett. 2020;473:139–47.
18. Lin C, Xu X, Yang Q, Liang L, Qiao S. Circular RNA ITCH suppresses proliferation, invasion, and glycolysis of ovarian cancer cells by up-regulating CDH1 via sponging miR-106a. Cancer Cell Int. 2020;20:336.
19. Zhang N, Yang Z, Jin Y, Cheng S, Yang J, Wang Y. Low Expression of Circular RNA hsa_circ_0078607 Predicts Poor Prognosis in High-Grade Serous Ovarian Cancer. Cancer Manag Res. 2021;13:2877–83.
20. Tang X, Liu S, Ding Y, Guo C, Guo J, Hua K, et al. Serum Circular FoxO3a Serves as a Novel Prognostic Biomarker in Squamous Cervical Cancer. Cancer Manag Res. 2020;12:2531–40.
21. Yin WB, Yan MG, Fang X, Guo JJ, Xiong W, Zhang RP. Circulating circular RNA hsa_circ_0001785 acts as a diagnostic biomarker for breast cancer detection. Clin Chim Acta. 2018;487:363–8.
22. Teng F, Xu J, Zhang M, Liu S, Gu Y, Zhang M, et al. Comprehensive circular RNA expression profiles and the tumor-suppressive function of circHIPK3 in ovarian cancer. Int J Biochem Cell B. 2019;112:8–17.
23. Robin X, Turck N, Hainard A, Tiberti N, Lisacek F, Sanchez J-C, et al. pROC: an open-source package for R and S + to analyze and compare ROC curves. BMC Bioinformatics. 2011;12:77.
24. Dudekula DB, Panda AC, Grammatikakis I, De S, Abdelmohsen K, Gorospe M. CircInteractome. A web tool for exploring circular RNAs and their interacting proteins and microRNAs. RNA Biol. 2016;13(1):34–42.
25. Liu M, Wang Q, Shen J, Yang BB, Ding X. Circbank: a comprehensive database for circRNA with standard nomenclature. RNA Biol. 2019;16(7):899–905.
26. Vilming Elgaaen B, Olstad OK, Haug KBF, Brusletto B, Sandvik L, Staff AC, et al. Global miRNA expression analysis of serous and clear cell ovarian carcinomas identifies differentially expressed miRNAs including miR-200c-3p as a prognostic marker. BMC Cancer. 2014;14:80.
27. Lewis BP, Shih Ih, Jones-Rhoades MW, Bartel DP, Burge CB. Prediction of mammalian microRNA targets. Cell. 2003;115(7):787–98.
28. Chen Y, Wang X. miRDB: an online database for prediction of functional microRNA targets. Nucleic Acids Res. 2020;48(D1):D127-D31.
29. Hansen TB, Jensen TI, Clausen BH, Bramsen JB, Finsen B, Damgaard CK, et al. Natural RNA circles function as efficient microRNA sponges. Nature. 2013;495(7441):384–8.
30. Du WW, Zhang C, Yang W, Yong T, Awan FM, Yang BB. Identifying and Characterizing circRNA-Protein Interaction. Theranostics. 2017;7(17):4183–91.
31. Shi Y, Jia X, Xu J. The new function of circRNA: translation. Clin Transl Oncol. 2020;22(12):2162–9.
32. Legnini I, Di Timoteo G, Rossi F, Morlando M, Briganti F, Sthandier O, et al. Circ-ZNF609 Is a Circular RNA that Can Be Translated and Functions in Myogenesis. Mol Cell. 2017;66(1):22–37.
33. Lei B, Zhou J, Xuan X, Tian Z, Zhang M, Gao W, et al. Circular RNA expression profiles of peripheral blood mononuclear cells in hepatocellular carcinoma patients by sequence analysis. Cancer Med. 2019;8(4):1423–33.
34. Reimers N, Pantel K. Liquid biopsy: novel technologies and clinical applications. Clin Chem Lab Med. 2019;57(3):312–6.
35. Dragomir M, Calin GA. Circular RNAs in Cancer - Lessons Learned From microRNAs. Front Oncol. 2018;8:179.
36. Li J, Song Y, Wang J, Huang J. Plasma circular RNA panel acts as a novel diagnostic biomarker for colorectal cancer detection. Am J Transl Res. 2020;12(11):7395–403.
37. Hu Y, Zhu Y, Zhang W, Lang J, Ning L. Utility Of Plasma circBNC2 As A Diagnostic Biomarker In Epithelial Ovarian Cancer. Onco Targets Ther. 2019;12:9715–23.

Ge *et al. Journal of Ovarian Research*   (2022) 15:58

Page 12 of 12

38. Wang W, Wang J, Zhang X, Liu G. Serum circSETDB1 is a promising biomarker for predicting response to platinum-taxane-combined chemotherapy and relapse in high-grade serous ovarian cancer. OncoTargets Ther. 2019;12:7451–7.

39. Kristensen LS, Jakobsen T, Hager H, Kjems J. The emerging roles of circRNAs in cancer and oncology. Nat Rev Clin Oncol. 2022;19(3):188–206.

40. Wolf D, Fiegl H, Zeimet AG, Wieser V, Marth C, Sprung S, et al. High RIG-I expression in ovarian cancer associates with an immune-escape signature and poor clinical outcome. Int J Cancer. 2020;146(7):2007–18.

41. Patel PS, Abraham KJ, Guturi KKN, Halaby MJ, Khan Z, Palomero L. dt al. RNF168 regulatesR-loop resolution and genomic stability in BRCA1/2-deficient tumors. J Clin Invest. 2021;131(3):e140105.

42. Nahand JS, Taghizadeh-Boroujeni S, Karimzadeh M, Borran S, Pourhanifeh MH, Moghoofei M, et al. microRNAs: New prognostic, diagnostic, and therapeutic biomarkers in cervical cancer. J Cell Physiol. 2019;234(10):17064–99.

43. Delangle R, De Foucher T, Larsen AK, Sabbah M, Azaïs H, Bendifallah S, et al. The Use of microRNAs in the Management of Endometrial Cancer: A Meta-Analysis. Cancers. 2019;11(6):832.

44. Giannopoulou L, Zavridou M, Kasimir-Bauer S, Lianidou ES. Liquid biopsy in ovarian cancer: the potential of circulating miRNAs and exosomes. Transl Res. 2019;205:77–91.

45. Chen LL. The biogenesis and emerging roles of circular RNAs. Nat reviews Mol Cell Biol. 2016;17(4):205–11.

46. Verduci L, Strano S, Yarden Y, Blandino G. The circRNA-microRNA code: emerging implications for cancer diagnosis and treatment. Mol Oncol. 2019;13(4):669–80.

47. Zhang F, Xu Y, Ye W, Jiang J, Wu C. Circular. RNA S-7 promotes ovarian cancer EMT via sponging miR-641 to up-regulate ZEB1 and MDM2. Biosci Rep. 2020;40(7):BSR20200825.

48. Li RC, Ke S, Meng FK, Lu J, Zou XJ, He ZG, et al. CiRS-7 promotes growth and metastasis of esophageal squamous cell carcinoma via regulation of miR-7/HOXB13. Cell Death Dis. 2018;9(8):838.

49. Weng W, Wei Q, Toden S, Yoshida K, Nagasaka T, Fujiwara T, et al. Circular RNA ciRS-7-A Promising Prognostic Biomarker and a Potential Therapeutic Target in Colorectal Cancer. Clin Cancer Res. 2017;23(14):3918–28.

50. Hansen TB, Kjems J, Damgaard CK. Circular RNA and miR-7 in cancer. Cancer Res. 2013;73(18):5609–12.

51. Li Y, Ge YZ, Xu L, Jia R. Circular. RNA ITCH: A novel tumor suppressor in multiple cancers. Life Sci. 2020;254:117176.

52. Luo L, Gao Y, Sun X. Circ-ITCH correlates with small tumor size, decreased FIGO stage and prolonged overall survival, and it inhibits cells proliferation while promotes cells apoptosis in epithelial ovarian cancer. Cancer Biomark. 2018;23(4):505–13.

53. Li Y, Zeng Qa, Qiu J, Pang T, Ye F, Huang L, et al. MiR-183-5p Promotes Proliferation, Metastasis and Angiogenesis in Breast Cancer Cells through Negatively Regulating Four and a Half LIM Protein 1. J Breast Cancer. 2020;23(4):355–72.

54. Wang L, Zhu MJ, Ren AM, Wu HF, Han WM, Tan RY, et al. A ten-microRNA signature identified from a genome-wide microRNA expression profiling in human epithelial ovarian cancer. PLoS ONE. 2014;9(5):e96472.

55. Lu F, Li C, Sun Y, Jia T, Li N, Li H. Upregulation of miR-1825 inhibits the progression of glioblastoma by suppressing CDK14 though Wnt/β-catenin signaling pathway. World J Surg Oncol. 2020;18(1):147.

56. Ren Z, He M, Shen T, Wang K, Meng Q, Chen X, et al. MiR-421 promotes the development of osteosarcoma by regulating MCPIP1 expression. Cancer Biol Ther. 2020;21(3):231–40.

57. Liu X, Li J, Yu Z, Li J, Sun R, Kan Q. miR-935 Promotes Liver Cancer Cell Proliferation and Migration by Targeting SOX7. Oncol Res. 2017;25(3):427–35.

58. Xue WX, Zhang MY, Rui L, Liu X, Yin YH, Qu YQ. Serum miR-1228-3p and miR-181a-5p as Noninvasive Biomarkers for Non-Small Cell Lung Cancer Diagnosis and Prognosis. Biomed Res Int. 2020;2020:9601876.

59. Du J, Xu R. RORα, a potential tumor suppressor and therapeutic target of breast cancer. Int J Mol Sci. 2012;13(12):15755–66.

60. Lee JM, Kim IS, Kim H, Lee JS, Kim K, Yim HY, et al. RORalpha attenuates Wnt/beta-catenin signaling by PKCalpha-dependent phosphorylation in colon cancer. Mol Cell. 2010;37(2):183–95.

61. Kim H, Lee JM, Lee G, Bhin J, Oh SK, Kim K, et al. DNA damage-induced RORα is crucial for p53 stabilization and increased apoptosis. Mol Cell. 2011;44(5):797–810.

62. Kumar S, Sharghi-Namini S, Rao N, Ge R. ADAMTS5 functions as an anti-angiogenic and anti-tumorigenic protein independent of its proteoglycanase activity. Am J Pathol. 2012;181(3):1056–68.

63. Wang W, Shen T, Dong B, Creighton CJ, Meng Y, Zhou W, et al. MAPK4 overexpression promotes tumor progression via noncanonical activation of AKT/mTOR signaling. J Clin Invest. 2019;129(3):1015–29.

64. Shen T, Wang W, Zhou W, Coleman I, Cai Q, Dong B, et al. MAPK4 promotes prostate cancer by concerted activation of androgen receptor and AKT. J Clin Invest. 2021;131(4):e135465.

65. Deborde S, Omelchenko T, Lyubchik A, Zhou Y, He S, McNamara WF, et al. Schwann cells induce cancer cell dispersion and invasion. J Clin Invest. 2016;126(4):1538–54.

66. Sasca D, Szybinski J, Schüler A, Shah V, Heidelberger J, Haehnel PS, et al. NCAM1 (CD56) promotes leukemogenesis and confers drug resistance in AML. Blood. 2019;133(21):2305–19.

67. Wen J, Liu J, Zhang P, Jiang H, Xin L, Wan L, et al. RNA-seq reveals the circular RNA and miRNA expression profile of peripheral blood mononuclear cells in patients with rheumatoid arthritis. Biosci Rep. 2020;40(4):BSR20193160.

68. Li J, Liu D, Wu K, Chen Q, Lei J. Circ_0003972 Promotes the Proliferation and Inflammation of Fibroblast-like Synovial Cells in Rheumatoid Arthritis through Regulation of the miR-654-5p/FZD4 Axis. Immunol Invest. 2021. https://doi.org/10.1080/08820139.2021.1958837.

69. Ma J, Meng Q, Zhan J, Wang H, Fan W, Wang Y, et al. Paeoniflorin Suppresses Rheumatoid Arthritis Development via Modulating the Circ-FAM120A/miR-671-5p/MDM4 Axis. Inflammation. 2021;44(6):2309–22.

Publisher's note

Springer Nature remains neutral with regard to jurisdictional claims in published maps and institutional affiliations.